16th World Conference on Earthquake, 16WCEE 2017

Santiago Chile, January 9th to 13th 2017

Paper N°1257

Registration Code: S-E1461885901

DESIGN AND BEHAVIOR OF BUCKLING RESTRAINED BRACES

A. S Jones[1], C-L. Lee[2] and G. A MacRae[3]

[1] *PhD Candidate, University of Canterbury, audsley.jones@pg.canterbruy.ac.nz*
[2] *Senior Lecturer, University of Canterbury, chin-long.lee@canterbury.ac.nz*
[3] *Associate Professor, University of Canterbury, gregory.macrae@canterbury.ac.nz*

Abstract

Buckling restrained braces (BRBs) have become a common and economic form of concentric bracing over the past decade. Used as the primary lateral load resisting system in high seismic areas, BRBs exhibit near balanced hysteresis loops, allowing for effective energy dissipation. Two forms of BRBs are commonly used, (i) a composite BRB composing of a steel core, surrounded by a concrete restraining medium and steel hollow section casing, and (ii) an all-steel BRB of a steel core surrounded by a steel restraining section(s). By restraining the steel core laterally along its length, the steel core can develop equal compression and tension capacity, and also suppress local buckling throughout the full brace length. Although simple in theory, BRBs are composed of five elements, three of which are defined segments along the core length; a yielding core, non-yielding restrained core, non-yielding unrestrained core, unbonding layer and restraining mechanism. The design and influence of these five elements is crucial in design of BRBs, a small imperfection or geometric change can significantly influence how the BRB behaves, in some cases in an explosive way. The purpose of this research is to understand the influence and contribution each element has in BRB design and also the sensitivity of variations in the detailing of these parameters to overall response.

This paper outlines the outcome of part one of a three part program addressing the design, sensitivity and behaviour of composite and all-steel BRBs as members and within a structural frame. Part one considers the effects the transition region and outer casing stiffness have on the overall brace performance and design. It was found that for smaller transition gradients, core local failure within the outer casing dominated, the compression strength was maintained at larger displacements and the maximum compression strength occurred after few loading cycles. For specimens with thinner outer casings (and subsequently lower stiffness) local buckling was sustained, rather than in-plane rotation at the connection. The compression strength was also maintained over larger displacements and a number of unstable cycles could be sustained before failure. Specimens with casings of a thickness equal to or greater than the steel core thickness fractured prematurely.

Keywords: buckling restrained brace; experimental testing; local buckling; in-plane rotation

1. Introduction

Buckling restrained braces (BRBs) have become a common and economic form of concentric bracing over the past decade. BRBs are commonly used as the primary lateral load resisting system due to their ability to exhibit near balanced hysteresis loops, allowing for effective energy dissipation and approximately equal tension and compression capacities. Two forms of BRBs are commonly used, (a) a composite BRB (Fig. 1) composing of a steel core surrounded by a concrete or grout restraining medium, and a steel hollow section casing and (b) a all-steel BRB composing of a steel core surrounded by one or more sections providing steel restraint.

By restraining the steel core laterally along its length, the steel core can develop similar compression and tension capacities, and also limit local buckling throughout the full brace length. It is common for the compression strength of a BRB to be greater than that in tension [1]. Although simple in theory, BRBs are composed of five elements, three of which are defined segments along the core length; a yielding core, non-yielding restrained core, non-yielding unrestrained core, unbonding layer and restraining mechanism. The design and influence of these five elements is crucial in design of BRBs. A small imperfection or geometric change can significantly influence how the BRB behaves. Due to intellectual property and the cost for experimental verification, little information is published concerning the design and sensitivity of the geometric elements that form the BRB. The purpose of this research is to understand the influence and contribution each element has in BRB design and also the sensitivity of variations in the detailing of these parameters to overall response.

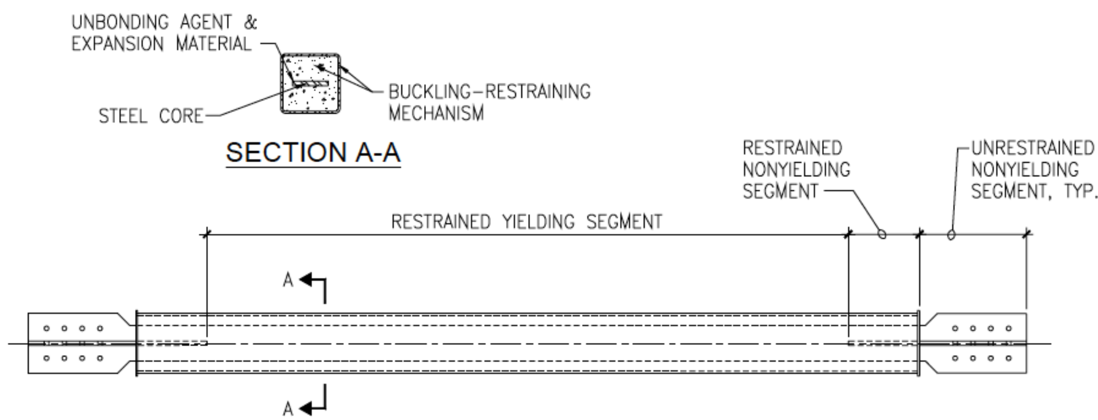

Fig. 1 – BRB Elements [2]

This paper outlines the outcome of part one of a three-part program addressing the design, sensitivity and behaviour of composite and all-steel BRBs as members and within a structural frame. This program was carried out in two parallel stages of numerical modelling and experimental testing.

Part one of the program consisted of experimental testing of 10 composite BRBs loaded concentrically. These have varying geometric details between the brace-to-gusset plate connection and the transition region which joins the yielding region to the non-yielding region. Also, there is different restraining medium stiffness and outer casing stiffness.

Part two considers concentric and eccentric BRB member tests. These members may be short or long, and they may be composite or all-steel specimens. The tests consider the effect of small variations in embedment length, transition region slope, and restraining medium stiffness influencing the propensity for local buckling and brace end restraint.

Part three addresses the behaviour of the BRB member within a structural frame in varying configurations (concentric, V and inverted V) and connection types (pin and bolted) while loaded in two horizontal directions. In conjunction with the experimental phase of the program, parametric analysis is considered through the development of a BRB numerical model.

The key questions to be answered within Phase one include:

1. How does the transition region affect brace performance and design?
2. What is the effect of casing thickness?

2. Specimen Design

2.1 Current Design Practice

The presence of BRBs in design guidelines is relatively new. The first recommendations were published in 2001 by The Structural Engineers Association of Northern California [3] who produced testing provisions, in which the BRB had to achieve at least two successful cyclic tests in two sub assemblage forms. These provisions also introduced guidance on designing the steel axial core (yielding region only) and also expressions for the strain hardening adjustment factor (ω), which accounts for material overstrength and strain hardening of the core, and the compression strength adjustment factor (β), which accounts for the difference in tension and compression capacities [3].

These recommendations were adopted by the National Earthquake Hazard Reduction Program (NEHRP) in 2003[4] and served as the only BRB design guidance for engineers. In 2010 these provisions were adopted in Section F4 and K3 of ANSI/AISC 341-10 “Seismic Provisions for Structural Steel Buildings” (AISC 2010) and are now code regulated within the United States of America [1].

Within the Eurocodes, no BRB design regulations are found. Commercial suppliers are complying with Eurocode 8, Part 1, “Design of structures for earthquake resistance” [5] Section 4.3.3.4.2.1, seismic no-collapse through non-linear static (pushover) or non-linear dynamic (time-history, response history) analysis [6] for design. European Standard EN 15129, “Anti-seismic devices” [7] includes the use of BRB among its displacement dependent devices; however no guidance or referral to design guidelines is cited.

Within New Zealand, design guidance is being developed to guide engineers in implementation of BRBs into new and existing structures. However, no guidance is currently being developed by industry for the design of the BRBs themselves. It is expected that all BRBs will be required to undergo experimental verification [1] however a number of in-house BRBs have been designed and implemented into New Zealand buildings without undergoing such testing, resulting in an unknown level of safety and uncertain behaviour under seismic loading [8].

2.2 Phase One Specimen Design

The specimens were designed based on current literature, codified provisions and BRB guidance documents available at the time of design. The premise of design was to mirror what an engineer would do with the available literature and provisions. All design was carried out to the minimum required within the New Zealand structural standards. The BRB specimen design was connection dependent and a detail of each region’s design is detailed in the following subsections.

2.2.1 Yielding Region Area

The yielding region area of the core is the most commonly specified design criteria within structural codes and literature. It is the area that defines the yielding capacity of the BRB, based on experimental testing a material and compression over-strength factor is applied to capture the true tension and compression capacity of the BRB. The larger the yielding region area, the less sensitive the BRB behavior is to geometrical variations. Based on this, and recommendations from a commercial supplier [9], a yielding region area close to 645 mm^2 (1 in^2) was chosen to adequately capture the BRB sensitivity in performance as a result of geometrical variations.

2.2.2 Yielding Region Length, L_y

The yielding region length is ideally taken as 2/3 the work-point to work-point (wp-wp) length of the brace (Fig. 2) [2]. This is dependent of the proportioning of the yielding region, transition region and non-yielding region (including connection) lengths. Within this study an ideal yielding length of 2.7 m (based on a wp-wp length of 4 m) was chosen for all specimens. However this was reduced to ~2.4 m on convergence of all three regions' lengths. This decrease in yielding length could reduce the susceptibility to global buckling and also allow for the energy dissipation to be distributed over the full yielding region. However as this length decreases it also results in greater localized plastic deformation. With an accumulation of plastic deformation, the susceptibility to low cycle fatigue increases and so does the brace susceptibility to local buckling in higher modes.

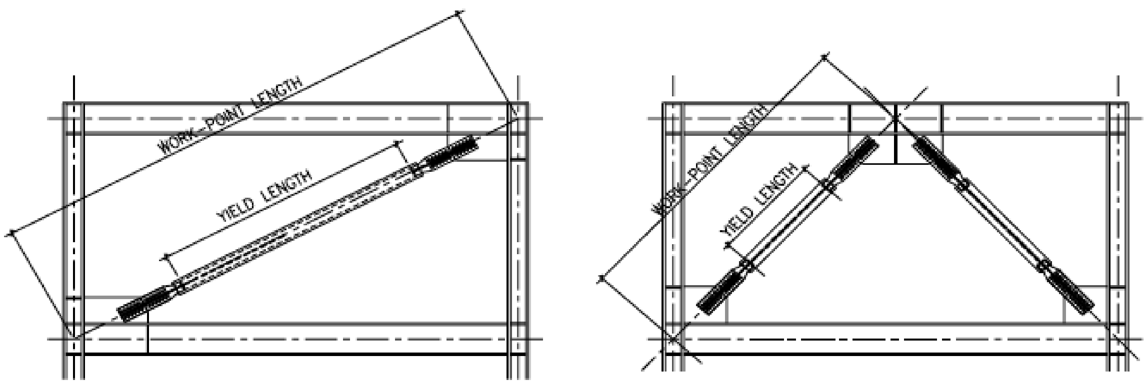

Fig. 2 – BRB work-point to work-point length [2]

2.2.3 Transition Gradient, TG, L_t

The transition gradient (TG) is the slope in which the yielding region transitions into the non-yielding region, and the transition length (L_t) is the subsequent length as a result of this gradient. This region is seldom detailed in literature except for the gradient used. The larger the gradient, the BRB will become more susceptible to stress concentrations, local buckling and end rotation. The minimum transition slope for notched regions stated in Clause 12.12.7.2 (e) of NZS 3404 is 1:2.5 (vertical:horizontal) [10]. Based on a review of commercial BRB designs [11], 1:3 and 1:4 slopes were commonly used and will be evaluated alongside 1:2.5 to measure any sensitivity to the gradient.

2.2.4 Non-yielding Length, L_{ny}

The non-yielding lengths (which comprise the restrained and un-restrained length) purpose is to prevent plastic deformation and/or high strains from accumulating outside the yielding length and also allow for the BRB to be connected to the surrounding frame. It is typically stiffened and also the embedment (restrained) portion of the region is key in preventing end rotations, and undesirable BRB-gusset plate interaction. The embedment length will be considered in Phase two of the experimental testing and will remain constant, approximately equal to the transition length in Phase one testing. The non-yielding region length was determined in conjunction with the yielding region length, by converging the remaining available length once the transition length was deducted. The unrestrained non-yielding portion was determined based on the expected frame drift at 2% and a brace-to-frame angle of 45° (Fig. 4) a worst-case scenario.

2.2.5 Unbonding Medium

Early development of BRBs consisted of a void separating the steel core from the restraining mechanism; this resulted in local buckling as a result of plastic strain concentrations affecting the hysteresis performance [12] and hence similar compression and tension capacities. It is common to use a material such as Teflon or lubricant as the unbonding material, which is sufficiently soft for transverse expansion of the core to occur [12]. Layers commonly vary from 0.15 mm to 2 mm and it has been found that the compression strength can be up to 35% greater than that of tensile by using different unbonding material [12, 13]. The unbonding medium used in this research is Denso tape, a neutral petrolatum compound [14]. This medium was previously used in BRB proof tests carried out at the University of Auckland and performed well [15].

2.2.6 Restraining Mechanism

The restraining mechanism for composite BRBs is a two-part system consisting of a restraining medium, typically grout, and a steel outer casing. In the original BRB research, conducted by Watanabe [16], it was proposed that the Euler critical buckling load of the outer casing should be greater than 1.5 times the core yield load. This ratio is commonly referred to in BRB design and considers the global, rather than local, buckling of the BRB.

The restraining mechanism contributes to limiting steel core local buckling, but little literature deals specifically with this. Takeuchi [17] proposed a method to calculated whether the restraining mechanism is appropriate or not in both the major and minor axes of the BRB. This method considers the flexural capacity of the restraining medium and the punching force (the force exerted on the inner outer casing surface as a result of the steel core “puncturing” through the restraining medium). This is a function of both the outer casing, and restraining medium, based on the assumption that the local buckling wavelength of the core plate is approximately four times the core plate width.

Lin et al. [18] proposed a similar relationship estimating the maximum outward (punching) force based on the geometrical characteristics of the high mode buckling length and available space between the steel core and the restraining mechanism. Both methods assume the restraining medium spreads the outward punching force to the outer casing inter surface, with Takeuchi proposing a mortar spread factor for both the major and minor axis. Lin et al. [18] proposed a demand-to-capacity ratio in which a thicker outer casing increases the resistance to the outward force. The thicker the unbonding medium, the greater the susceptibility to local buckling. Also, the closer the outer casing depth is to the core plate depth, the greater the resistance to local buckling failure.

In Phase one of this program, the proposed Euler critical buckling load ratio is investigated, with the restraining medium contribution investigated within Phase two. The outer casings of the specimens were proportioned for the constant, *a*, to be either equal to 1.5 or 2.0, in Equation (1).

$$P_{core} = \frac{P_{Euler\,casing}}{a} \tag{1}$$

2.2.7 Connection

A pin connection with full rotation was chosen for each specimen. The pin connection was chosen due to the ability for the BRB to transfer force without any additional strain or rotations building at the connection. This allows the behaviour of the BRB to be isolated to identify any sensitivity present from the variable parameters. A flush form pin with external gussets was used for each specimen, eliminating the use of welds to connect the BRB to the pin connector and for ease of attachment to the loading apparatus. By eliminating the need for welds, the required width of the flush form pin dictated the non-yielding width and as a consequence the transition length.

2.2.8 Specimen Summary

Table 1 summarizes the key geometric and material features for each specimen tested. The steel core was specified as AS/NZS 3678-250S0 steel (250 MPa seismic grade) and the outer casing AS/NZS 3679-300S0 steel (300 MPa seismic grade). 3 mm Denso tape, a neutral petrolatum compound [14] was applied as the unbonding layer, and Sika Grout 215 for the restraining medium. Sika Grout 215 is a specialty grout used in voids with narrow dimension (3-4 mm) and contains additives to prevent shrinkage and the need for vibration [19].

Table 1 – Specimen Key Design Features

Design feature	**Specimen**									
	1	**2**	**3**	**4**	**5**	**6**	**7**	**8**	**9**	**10**
Core thickness (mm)	12	12	12	12	12	12	12	12	12	12
Specified yielding width (actual yielding width) (mm)	50 (38)	50 (38)	50 (38)	50 (38)	50 (38)	50 (38)	50 (38)	50 (38)	50 (38)	50 (38)
Non-yielding width (mm)	160	160	160	160	160	160	160	160	160	160
Yielding length, L_y (mm)	2420	2420	2470	2330	2420	2420	2420	2470	2330	2420
Transition length, L_t (mm)	170	170	140	220	170	170	170	140	220	170
Non-yielding length (excluding connection length), L_{ny} (mm)	170	170	175	165	170	170	170	175	165	170
BRB length, L_{BRB} (mm) $L_{BRB} = L_y + (2 \times L_t) + (2 \times L_{ny})$	3100	3100	3100	3100	3100	3100	3100	3100	3100	3100
Casing thickness (mm)	5	8	8	8	10	6	8	8	8	10
Casing width (mm)	180	180	180	180	190	180	180	180	180	190
Casing depth (mm)	45	45	45	45	45	50	50	50	50	50
Transition gradient, TG (vertical:horizontal)	1:3	1:3	1:2.5	1:4	1:3	1:3	1:3	1:2.5	1:4	1:3
$\frac{P_{Eulercasing}}{1.5\times P_{core}}$ **specified (actual)**	0.763 (1.00)	1.04 (1.37)	1.04 (1.37)	1.04 (1.37)	1.23 (1.62)	-	-	-	-	-
$\frac{P_{Eulercasing}}{2.0\times P_{core}}$ **specified (actual)**	-	-	-	-	-	0.834 (1.10)	1.01 (1.33)	1.01 (1.33)	1.01 (1.33)	1.20 (1.58)
Grout, f'_c (MPa)	48.7	34.5	40.6	37.0	34.4	38.8	37.6	41.0	39.9	35.2

Note: High values of $\frac{P_{Eulercasing}}{\alpha\times P_{core}}$ are conservative

3. Specimen Fabrication

Due to the design of the connection, packing plates were required at each end of the BRB after the core had been placed in the casing. Fabrication was applied in two stages. Stage one consisted of applying the unbonding medium to the core, placing the casing appropriately over the core, and welding a cap plate at the bottom end to hold the casing in place, and welding packing plates at each end. Stage two consisted of suspending (Fig. 3) the specimens vertically and aligning the casings to the core, applying a pre-tensioning weight and pumping the grout into each specimen. All specimens remained pre-tensioned for at least 24 hours after grout pumping to allow the grout to cure in place.

Along with specimen fabrication, grout cylinders for compression tests were taken for each specimen and also additional cylinders for batch testing at 21 and 28 days. The specimen cylinders were tested within one hour of completion of the BRB specimen tests, to capture the grout compression strength at time of testing.

The steel cores were provided by the supplier with a yielding width smaller than that specified. Due to laboratory timetabling constraints, these were used in the test specimens but they resulted in a 30% capacity reduction. This error affected the outer casing variable specified in Table 1 with the actual values shown in brackets.

Fig. 3 – BRB specimen vertical suspension

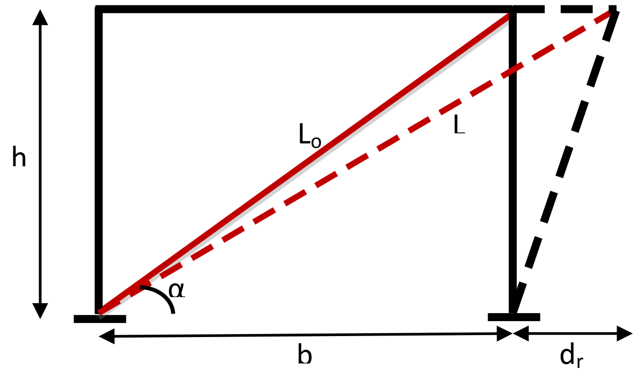

Fig. 4 – Design story drift calculation frame

4. Experimental Testing

Experimental testing was carried out on all 10 specimens using the loading protocol specified in Section 4.1 and the same testing set up for each test. All specimens were loaded within the Dartec vertical loading machine within the University of Canterbury Structures Laboratory, New Zealand. The 38 tonne Dartec has a maximum force (tension and compression) of 10 MN, actuator stoke of 300 mm and a maximum sustained velocity of 16 mm/s. All specimens were loaded at a rate of 0.5 mm/s to avoid strain effects and allow for at least four loading steps until first yield.

4.1 Loading Protocol

The loading protocol was determined based on the evaluation of proprietary system reports, codified specifications and previous research carried out for the development of codified specifications for the United States of America, Europe and Canada [1, 4, 7, 20].

The AISC 341-10 loading sequence was determined to be the most suitable and taxing on the specimens [1]. The loading sequence requires each specimen to achieve ductility's corresponding to 2.0 times the design story drift and a cumulative inelastic ductility capacity of 200 times the yield displacement. The loading sequence continues with additional cycles at 1.5 times the design story drift until failure, if required

The specimen first yield was determined using the steel core mill certificate specified yield strength (297 MPa) and by taking the yielding region plus 2/3 contribution (to the centroid) of each transition length as the buckling length. The transition length contribution is included as yielding can still occur within the region as the stresses distribute, it is assumed that the non-yielding region commences at the centroid of this region. The displacement at first yield (δ_y) for each specimen is 4mm.

The deformation at design story drift ($d_r = \Delta_{bm}$) was calculated using a worst-case frame (Fig. 4) with α = 45°. AISC 341-10[1] specifies that the design story drift shall not be taken as less than 0.01 times the story height (h). For the purposes of this study, Δ_{bm} was taken as 0.01 times the story height, h, of 2.83m which is 0.01 x 2.83m = 28mm (Fig. 5). The peak displacement (δ) in the loading regime therefore corresponds to a brace ductility, δ/δ_y, of 57mm/28mm = 2.0.

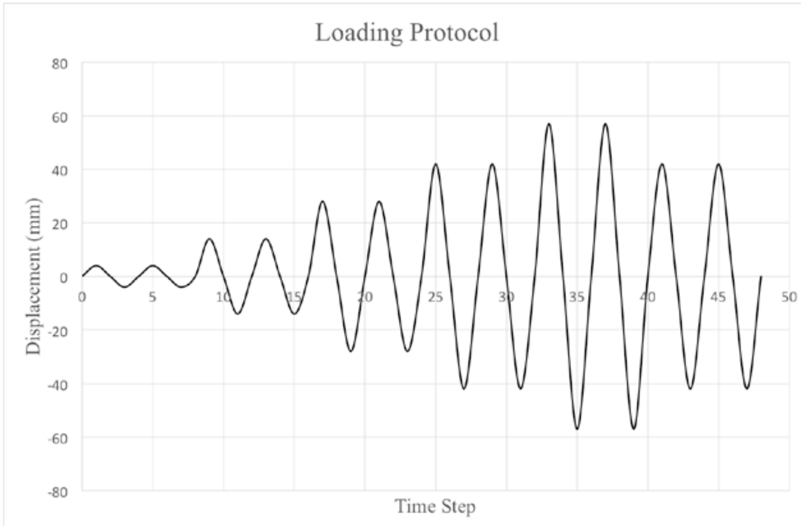

Fig. 5 – Applied loading protocol (δ_y = 4 mm)

4.2 Experimental Testing Observations

In all tests a creaking sound occurred during the initial compression loading of the specimens above 0.5 times the design story drift. This creaking was followed, in all but two specimens, with casing movement. The casing typically moved down and settled on the connection packing plate. It moved only slightly during unloading. No specimens retained the outer casing at the position of casting. Once the casing had settled, it was common to hear creaking during the transition (unloading) from the compression to tension cycle, due to the new position of the outer casing and relief of pressure. The grout compression strength ranged between 34 MPa and 49 MPa for all specimens (Table1).

Fig. 6 – Yielding core fracture and fold onto transition region

Local buckling occurred in 6 out of 10 specimens and was random in location with respect to the top and bottom of the specimen. In all cases local buckling occurred in the quarter of the yielding core closest to the transition region indicating an end region effect. In many cases failure occurred by folding (Fig. 6) of the yielding core on the transition region. It was observed that each specimen underwent instability in the compression cycle and failed on unloading or underwent subsequent unstable cycles. All specimens were unable to achieve balanced hysteresis loops up to cumulative inelastic ductility capacity of 200 times the yield displacement.

5. Results

A summary of the key results can be found in Table 2, with normalized force-displacement graphs for each specimen in Fig. 7. Failure modes were (i) local buckling inside the yielding core and (ii) in-plane rotation, where the pin connection hinged with the transition region and rotated in plane. All local buckling failure was visible as the outer casing deformed at the crests (and troughs) of the core buckling wave. Specimen 3 underwent both in-plane rotation, local buckling, and failure in fracture of the non-yielding region that separated fully from the specimen on removal.

Table 2 – Behaviour summary

Specimen	F_y (kN)	T_{max} (kN)	C_{max} (kN)	Initial rotation (rad)	Failure mode	Cumulative inelastic ductility	No. stable cycles	No. unstable cycles
1	101	151	147	0.0320	Local buckling	362	5	9
2	101	163	250	0.0179	In-plane rotation	144	8	0
3	98.8	163	219	0.0000	Local buckling, In-plane rotation	196	8	1
4	98.8	161	188	0.0400	Local buckling	196	7	2
5	107	157	244	0.0360	In-plane rotation	68	5	1
6	96.9	155	163	0.0360	Local buckling	196	6	3
7	96.9	161	294	0.0089	In-plane rotation	106	7	0
8	101	167	201	0.0534	Local buckling	248	8	2
9	96.9	147	147	0.0000	Local buckling	106	4	3
10	101	157	157	0.0268	In-plane rotation	68	2	0

Note: Initial rotation is the out of placement (rad) between the ram head and connection base plate present before testing
Cumulative inelastic ductility (total of stable and unstable cycles) calculated in accordance with Table C-K3.1, ANSI/AISC 341-10 [1]

Specimen 1 underwent 5 stable cycles and 9 unstable cycles as shown in Fig. 7a. Stable cycles were defined as those where the force-displacement profile was balanced throughout the loading cycle. The specimen underwent local buckling of the core in the minor axis failing in compression. This specimen, although suffering from significant compression strength degradation in the unstable cycles, maintained tension capacity until failure. The thin casing was highly deformable and allowed the core to deform until the capacity of the core was less than that of the casing and restraining medium. This specimen has the highest grout compression strength of all specimens and this along with the thin casing likely contributed to the higher mode of local buckling failure. The tension and compression strength were comparable and the Euler buckling ratio for the casing of approximately 1.0 was insufficient to restrain the yielding core.

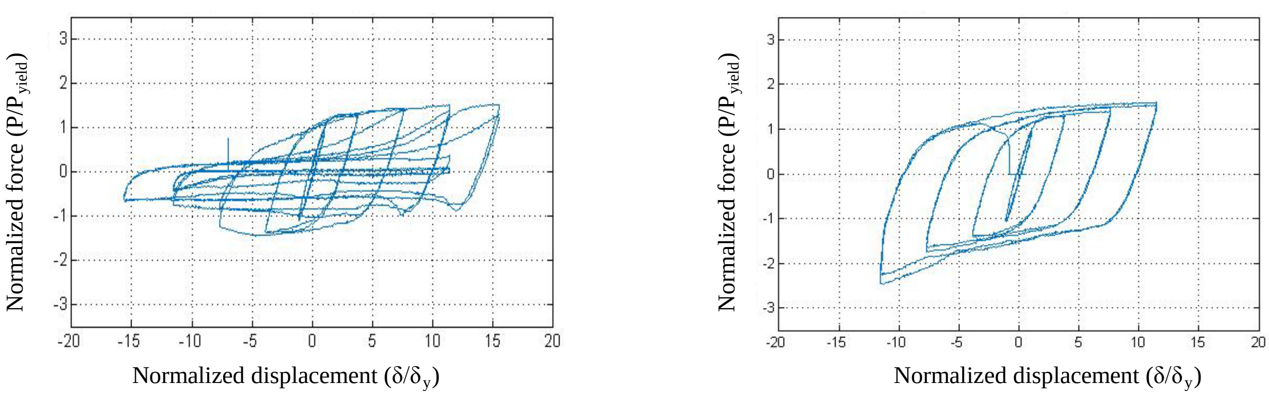

a) Specimen 1 (TG = 1:3, t_c = 5mm)

b) Specimen 2 (TG = 1:3, t_c = 8mm)

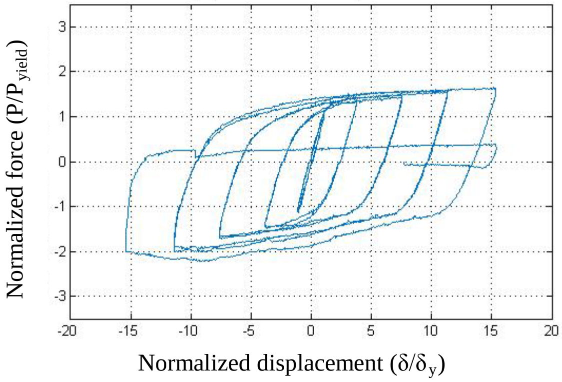

c) Specimen 3 (TG = 1:2.5, t_c = 8mm)

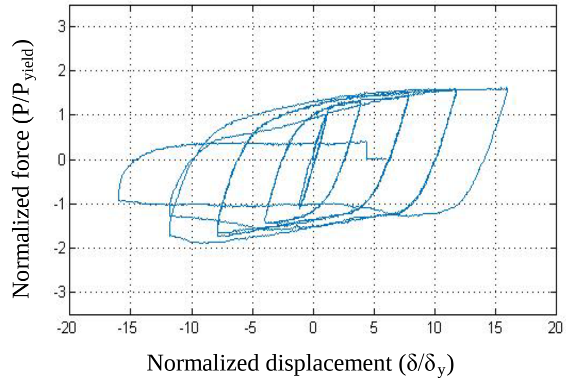

d) Specimen 4 (TG = 1:4, t_c = 8mm)

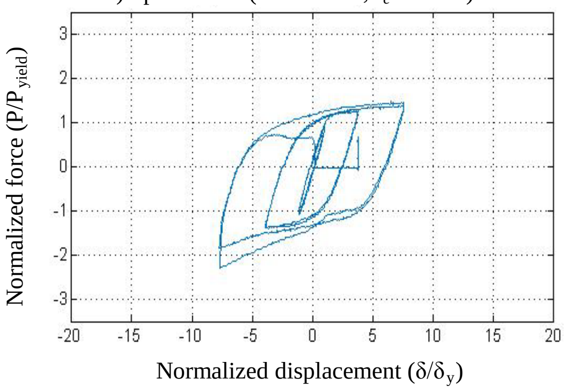

e) Specimen 5 (TG = 1:3, t_c = 10mm)

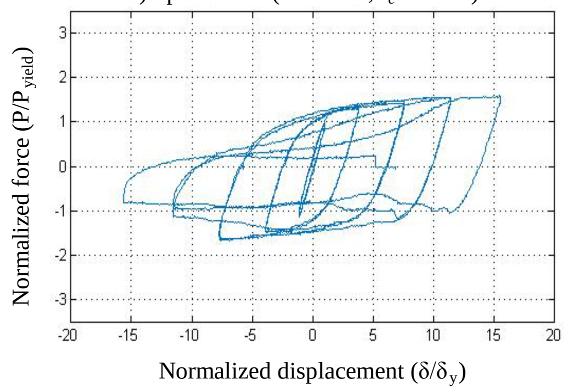

f) Specimen 6 (TG = 1:3, t_c = 6mm)

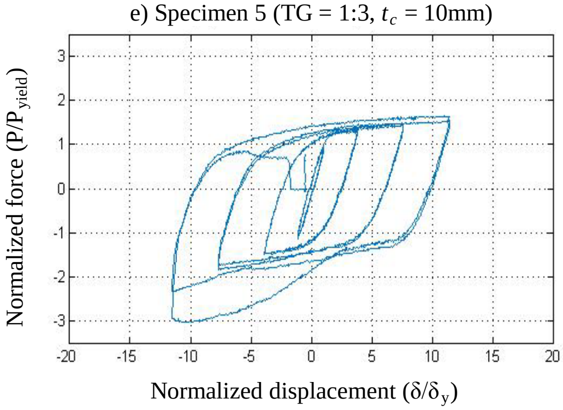

g) Specimen 7 (TG = 1:3, t_c = 8mm)

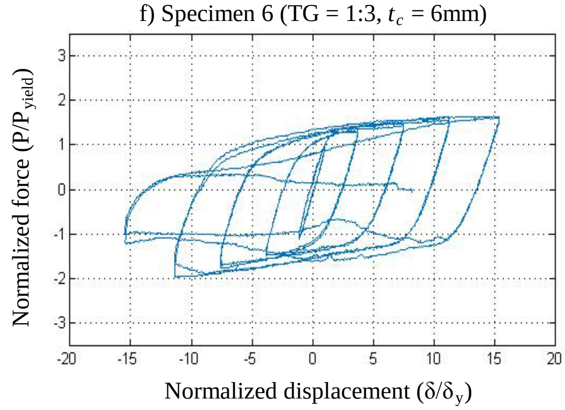

h) Specimen 8 (TG = 1:2.5, t_c = 8mm)

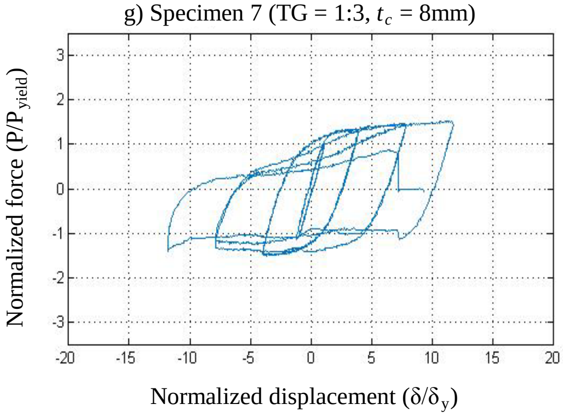

i) Specimen 9 (TG = 1:4, t_c = 8mm)

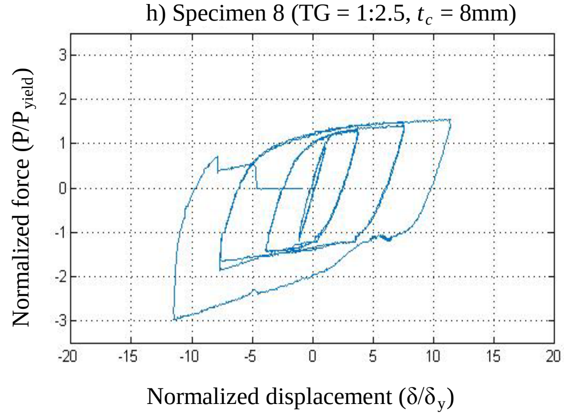

j) Specimen 10 (TG = 1:3, t_c = 10mm)

Fig. 7 – Normalized force verses normalized applied displacement (δ_y = 4mm, Δ_{bm} = 28mm)

Specimens 2, 3 and 4, all with identical casings varied in design by transition gradient, and subsequently yielding length, performed alike (Fig. 7b, c and d). It was found the longer the transition length (Specimen 4, TG = 1:4), the lower the maximum compression capacity and the greater the susceptibility to local buckling (Fig. 7d). The shorter the transition length (Specimen 3, TG = 1:2) the greater the stability throughout the loading sequence (Fig. 7c), even throughout local buckling. Specimen 2 underwent in-plane rotation and localized local buckling at one end, failing in the unloading sequence from compression to tension. Specimen 2 (Fig. 7b, TG = 1:3) with a transition length between Specimen 3 and 4 achieved the highest compression capacity of the three specimens, and failed in tension after two cycles of instability in compression.

Specimen 5 (TG = 1:3), with a thicker casing stiffness of 10mm sustained very few cycles, however reached significantly high maximum compression strength (Fig. 7e). This specimen underwent in-plane rotation failure, with instability occurring in the final compression cycle. Specimen 10 (TG = 1:3), also with a 10mm casing, behaved in a similar manner to Specimen 5 (Fig. 7j), failing in in-plane rotation, and undergoing significant instability within the final compression cycle, however the maximum tension and compression capacities were approximately equal. This behaviour is likely a function of the outer casing thickness being higher than that of the other specimens, and approximately equal to that of the steel core, This seemed to limit the possibility of local buckling, and inelastic deformation in that mode, so in-plane buckling became significant (rotation of the core in-plane at the connection), even though the in-plane buckling likelihood seemed less likely based on the ratio calculated. The deformation capacity in in-plane buckling seems to be significantly less than when local buckling occurs. What seems to be important here is the ratio of local buckling to lateral buckling propensity, when lateral buckling is not prevented.

Specimen 6 (TG = 1:3) with an identical core to Specimen 1 and stiffer outer casing performed similar to Specimen 1. The specimen underwent 6 stable cycles and 3 unstable (Fig. 7f). This specimen underwent local buckling of the core in the minor axis, failing in tension. Although suffering strength degradation throughout the loading cycles, the tension strength remained consistent, with the overall maximum compression and tension strength varying by 5% during the stable cycles.

Specimens 7, 8 and 9 (alike Specimens 2, 3 and 4), all with identical casings varied in design by transition gradient, and subsequently yielding length. Specimen 7 (Fig. 7g, TG = 1:3), similar to Specimen 2, failed in in-plane rotation and also achieved the greater compression capacity of the three specimens. There was instability in the final compression cycle prior to failure, likely a result of the in-plane rotation occurring at the connection. Specimen 8 (Fig. 7h, TG = 1:2.5) maintained stability until instability occurred in both tension and compression. Specimen 8 failed through the yielding core folding onto the transition region (Fig. 6). Specimen 9 (TG = 1:4), became unstable in both tension and compression after two successful cycles above yield (Fig. 7i). The maximum tension and compression capacity was approximately equal during the stable cycles. The trends in specimens 7, 8 and 9 were the same as that for Specimens 2, 3 and 4 probably for identical reasons.

6. Conclusions

Ten BRB specimens with steel cores encased in concrete-filled rectangular tubes were tested under cyclic inelastic deformation. It was found that:

1. For smaller transition gradients, and subsequently longer yielding regions,
   a. core local buckling within the casing, rather than in-plane brace rotation, dominated
   b. the compression strength was maintained at larger displacements,
   c. the maximum compressive strength occurred after fewer cycles, possibly because local buckling increased the strength
2. Braces with thinner outer casings
   a. sustained local buckling, rather than in-plane brace rotation and subsequent fracture

b. maintained compression strength at larger displacements, and maintained a number of unstable cycles before failure

c. had compression strengths less than 5% greater than the tensile strength, compared to 30% for thicker casings,

7. Acknowledgements

Special thanks to the financial contributors to this research: University of Canterbury College of Engineering Safe Building Doctoral Scholarship, University of Canterbury Quake Centre, BRANZ assistance from the Building Research Levy, the Heavy Engineering Education Research Foundation (HEERF).

8. References

[1] Construction, A.I.o.S., ANSI/AISC 341-10 Seismic Provisions for Structural Steel Buildings. 2010, AISC.

[2] W.A Lopez, R.S., Seismic Design of Buckling-Restrained Braced Frames. 2004, Technical Information and Product Service.

[3] California, S.E.A.o.N., Recommended Provisions for Buckling-Restrained Braced Frames. 2001.

[4] Provisions, P.o.I.S.S., NEHRP Recommended Provisions for Seismic Rwgulations for New Buildings and Other Structures (FEMA 450), B.S.S. Council, Editor. 2003, National Institute of Building Services: Washington, D.C.

[5] Institute, B.S., BS EN 1998-1:2004 Eurocode 8: Design of structures for earthquake reisitance, in Part 1: General rules, seismic actions and rules for buildings. 2004, British Standards Institute: London, United Kingdom.

[6] Ltd., S.S.E., Cost advantages of Buckling Restrained Braced Frame buildings in accordance with Eurocode. 2010.

[7] Comittee, E.S., EN 15129:2009 Anti-seismic devices. 2010.

[8] A. S Jones, C.-L.L., G. A MacRae, G. C Clifton, Review of buckling restrained brace design and behaviour, in New Zealand Society of Earthquake Engineering. 2014: Auckland, New Zealand.

[9] Jones, A.S., Core yeilding area sensitivity range. 2014.

[10] Zealand, S.N., NZS 3404 Steel Structures Standard. 1997, Standards New Zealand: Wellington.

[11] Jones, A.S., Commercial Buckling Restrained Brace Design Review. 2014.

[12] G. D Corte, M.D.A., R. Landolfo, F. M Mazzolani, Review of steel buckling-restrained braces. Steel Construction, 2011. **4**(2): p. 85-93.

[13] K. C Tsai, J.W.L., Y.C Hwang, S.L Lin, C.H Weng, Research and application of double-core buckling restrained braces in Taiwan. 13th World Conference on Earthquake Engineering, 2004.

[14] Denso, Technical Data Sheet Denso Tape. 2011.

[15] Wijanto, S., Behaviour and Design of Generic Buckling Restrained Brace Systems, in Department of Civil and Environmental Engineering. 2012, Univeristy of Auckland: Auckland.

[16] A. Watanabe, Y.H., E. Saeki, A. Wada, M. Fujimoto, Properties of brace encased in buckling-restraining concrete and steel tube. Proceedings of the Ninth World Conference on Earthquake Engineering, 1988.

[17] Takeuchi, T., et al., Effect of local buckling core plate restraint in buckling restrained braces. Engineering Structures, 2012. **44**(0): p. 304-311.

[18] P-C Lin, K.-C.T., C-A, Chang, Y-Y Hsiao, A-C Wu, Seismic design and testing of buckling-restrained braces with a thin profile. Earthquake Engineering and Structural Dynamics, 2015(45): p. 339-358.

[19] Sika, Sika Grout 212, 215 2012, Sika.

[20] Inc, I.E.S., Acceptance criteria for buckling-restrained brace frame subassemblages, in AC238. 2003, ICC.